Calculated fission-fragment yield systematics in the region $74 \leqslant Z \leqslant 94$ and $90 \leqslant N \leqslant 150$

Peter Möller[1,*] and Jørgen Randrup[2]
[1]*Theoretical Division, Los Alamos National Laboratory, Los Alamos, New Mexico 87545, USA*
[2]*Nuclear Science Division, Lawrence Berkeley National Laboratory, Berkeley, California 94720, USA*
(Received 27 June 2014; published 20 April 2015)

Background: In the seminal experiment by Schmidt *et al.* [Nucl. Phys. A **665**, 221 (2000)] in which fission-fragment charge distributions were obtained for 70 nuclides, asymmetric distributions were seen above nucleon number $A \approx 226$ and symmetric ones below. Because asymmetric fission had often loosely been explained as a preference for the nucleus to always exploit the extra binding of fragments near ^{132}Sn it was assumed that all systems below $A \approx 226$ would fission symmetrically because available isotopes do not have a proton-to-neutron Z/N ratio that allows division into fragments near ^{132}Sn. But the finding by Andreyev *et al.* [Phys. Rev. Lett. **105**, 252502 (2010)] did not conform to this expectation because the compound system ^{180}Hg was shown to fission asymmetrically. It was suggested that this was a new type of asymmetric fission, because no strong shell effects occur for any possible fragment division.
Purpose: We calculate a reference database for fission-fragment mass yields for a large region of the nuclear chart comprising 987 nuclides. A particular aim is to establish whether ^{180}Hg is part of a contiguous region of asymmetric fission, and if so, its extent, or if not, in contrast to the actinides, there are scattered smaller groups of nuclei that fission asymmetrically in this area of the nuclear chart.
Methods: We use the by now well benchmarked Brownian shape-motion method and perform random walks on the previously calculated five-dimensional potential-energy surfaces. The calculated shell corrections are damped out with energy according to a prescription developed earlier.
Results: We have obtained a theoretical reference database of fission-fragment mass yields for 987 nuclides. These results show an extended region of asymmetric fission with approximate extension $74 \leqslant Z \leqslant 85$ and $100 \leqslant N \leqslant 120$. The calculated yields are highly variable. We show 20 representative plots of these variable features and summarize the main aspects of our results in terms of "nuclear-chart" plots showing calculated degrees of asymmetry versus N and Z.
Conclusions: Experimental data in this region are rare: only ten or so yield distributions have been measured, some with very limited statistics. We agree with several measurements with higher statistics. Regions where there might be differences between our calculated results and measurements lie near the calculated transition line between symmetric and asymmetric fission. To draw more definite conclusions about the accuracy of the present implementation of the Brownian shape-motion approach in this region experimental data, with reliable statistics, for a fair number of suitably located additional nuclides are clearly needed. Because the nuclear potential-energy structure is so different in this region compared to the actinide region, additional experimental data together with fission theory studies that incorporate additional, dynamical aspects should provide much new insight.

DOI: 10.1103/PhysRevC.91.044316 PACS number(s): 25.85.Ca, 24.10.Lx, 24.75.+i, 25.85.Jg

I. INTRODUCTION

The discovery that fission of ^{180}Hg at low excitation energies ($E^* < 10$ MeV) results in an asymmetric fragment-mass distribution [1] has led to a flurry of theoretical and experimental studies [2–5]. There are few theoretical approaches that can routinely be applied to basically all fissioning systems and which show substantial agreement with observations. There are several approaches in terms of "scission-point" models but they normally have several parameters that are adjusted to experimental yield distributions. The very popular computer program and model GEF [6,7] describes more than fission yields, but introduces a large number of assumptions and contains a substantial number of parameters that are adjusted to experimental data. Outside regions where experimental data are available, it is unable to run, so, for example, it cannot presently produce a mass-yield curve for fission of ^{180}Hg.

The Brownian shape-motion model [8–10], on the other hand, has in its initial implementation [8] no adjustable parameters. There are two parameters, the strength of the bias potential and the critical neck radius, at which we assume that the fission-fragment mass asymmetry is frozen in. Since we have shown that the results are insensitive to a large range of these parameters [9], these parameters are not in the category of adjustable parameters. In the version of the model we use here, there are two adjustable parameters that govern the rate at which the shell effects are damped out with energy [10]. However, our main conclusions in this paper are not affected by how the damping of the shell effects is treated because the excitation energy is so low. For example, we obtain about the same mass yield for fission of ^{180}Hg and nearby isotopes without damping shell effects with energy [11], as we do here where we do include such an effect. The model has been extensively benchmarked, in Ref. [10] with respect to

*moller@lanl.gov

70 charge yields measured at GSI [12] and in Ref. [13] with respect to new and older data in the neutron-deficient Pb region.

As discussed in detail earlier [9], the Brownian shape-motion model constitutes a particularly simple approximate solution to the Langevin description of the nuclear shape dynamics, ignoring entirely the inertial effects and assuming that the dependence of the fission-fragment mass distribution is sufficiently insensitive to the structure of the dissipation tensor to render the Metropolis results useful. The Langevin transport framework has been employed extensively to fission dynamics ever since fission was discovered. The earliest numerical studies of dissipation in fission dynamics were focused on the damping effect on the mean motion only, using various physical models for dissipation, including inertial effects, and using macroscopic potentials [14–17]. Consideration of the stochastic force in fission dynamics began as early as 1940, when Kramers considered the average delay in establishing a stationary flow rate over a one-dimensional barrier, thus inferring an increase of the fission lifetime due to dissipation [18]. Further approximate treatments of the Fokker-Planck equation in one or two dimensions began around 1980 [19–23]. These calculations often retained the assumption of constant inertia and dissipation, using very simplified potentials. About a decade later, numerical investigations of Langevin equations for dynamics including inertia, damping, and Markovian stochastic forces were begun by several groups; reviews of such work were given in Refs. [24,25]. These types of simulations continue [26–30]. They employ two or three shape degrees of freedom, macroscopic potential energies, and fluid dynamic inertias. More recent calculations usually use some form of one-body dissipation. Because of the use of macroscopic energies, they are often explicitly characterized as applying to systems with significant excitation energy. Most recently, Aritomo and collaborators have made a number of fission studies of uranium and plutonium isotopes at $E^* =$ 20 MeV using a Langevin treatment that includes shell and pairing effects in a three-dimensional shape parametrization [31–33].

II. CALCULATIONAL DETAILS

We obtain 987 fission-fragment mass yields by performing random walks on previously calculated five-dimensional (5D) potential-energy surfaces, as described in Ref. [10]. The surfaces are tabulated on a discrete grid of more than 5 million points. We implement a damping of the shell-plus-pairing corrections with excitation energy as described in Ref. [10]. In contrast to previous work in the actinide region where we started the random walks in the fission-isomeric minimum [8], we here start the random walks in the nuclear ground-state minimum because many nuclides do not have fission-isomer minima. But since we only calculated potential-energy surfaces for elongations larger than about $\beta_2 = 0.10$ our surfaces do not contain the ground-state minima for nuclei such as ^{208}Pb. In those cases we start our calculation at the location with the lowest energy at the smallest elongation. This means we start at a point corresponding to a slightly more elongated shape than the ground state, that is slightly up the barrier with respect to the ground state. We have checked that we obtain practically identical yields for actinides whether we start at the ground state or at the fission-isomer minimum, so our results will not be affected by the missing spherical minimum.

Barriers for the lighter nuclides in our study here have very extended, flat saddle regions; see Ref. [34] for some examples. It is then very time-consuming for the Metropolis random-walk algorithm to cross the saddle region, because forward and backward steps are almost equally likely. To "nudge" it in the fission direction we have previously introduced a bias potential [8], which slightly tilts the surface in the fission direction, in particular for smaller elongations inside the fission saddle point. The strength of the bias potential was taken to be 15 MeV in Ref. [8]. However, with this strength it can take weeks to complete the 10 000 tracks we need to accumulate to obtain good statistics for some nuclides below Pb in the nuclear chart. We therefore use a bias potential strength of 60 MeV in our studies here. The differences in the results between the two choices are insignificant. Even with this choice, some yield calculations take several days for the lightest systems, whereas the time to complete a calculation for, say ^{240}Pu, is about one minute.

We aim to study situations where shell structure can be expected to govern the outcome the most, so we perform our calculations for excitation energies just a little above the barrier. This type of fission occurs in thermal-neutron-induced fission in many actinide nuclei [8] and in fission following β^--decay and electron capture (EC) [35]. In nuclides with higher barriers fission is induced in, for example, fragmentation reactions, proton capture, or heavy-ion reactions. In these reactions fission events are usually not observed very near the barrier but at energies corresponding to 5 or 10 MeV above the saddle-point energy; see, for example, Refs. [36,37]. We have available calculated barriers B_f for 5239 nuclides in Refs. [38,39]. The following algorithm reasonably approximates the lowest energy for which fission events can be observed (with units in MeV):

$$\begin{aligned} E^* &= B_f + 2 && \text{for } B_f < 10, \\ E^* &= B_f + 2 + (B_f - 10) \times 0.6 && \text{for } B_f > 10, \end{aligned} \tag{1}$$

and is used to determine the excitation energies in our calculations.

III. RESULTS

Our aim with the calculations is threefold: (1) to provide a reference database of fission-fragment mass yields, in particular in regions where experimental data currently are sparse; (2) to discuss how our results compare to the (few) data sets than are available in the neutron-deficient Pb region; and (3) to learn if the calculated yields suggest some particularly interesting studies.

In Figs. 1 and 2 we show the calculated fission-fragment mass yields for twenty selected isotopes, which are discussed below.

To find some possibly interesting fission reactions to propose as candidates for future experiments we checked if in the lighter region there are compound systems with $Z/N \approx 50/82$ that in addition are near stability. Such systems could exploit the exact double magicity that would occur in

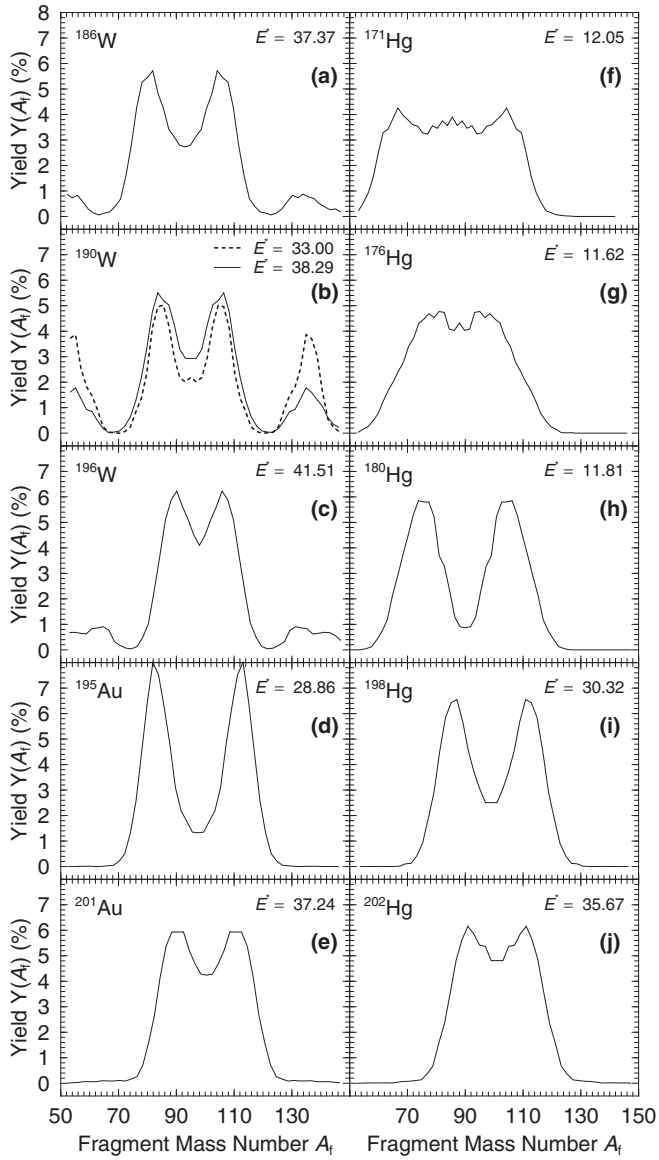

FIG. 1. Calculated fission-fragment mass yields for 10 isotopes of W, Au, and Hg. The compound-nucleus excitation energies E^* are in units of MeV. Details of these distributions are discussed in the text.

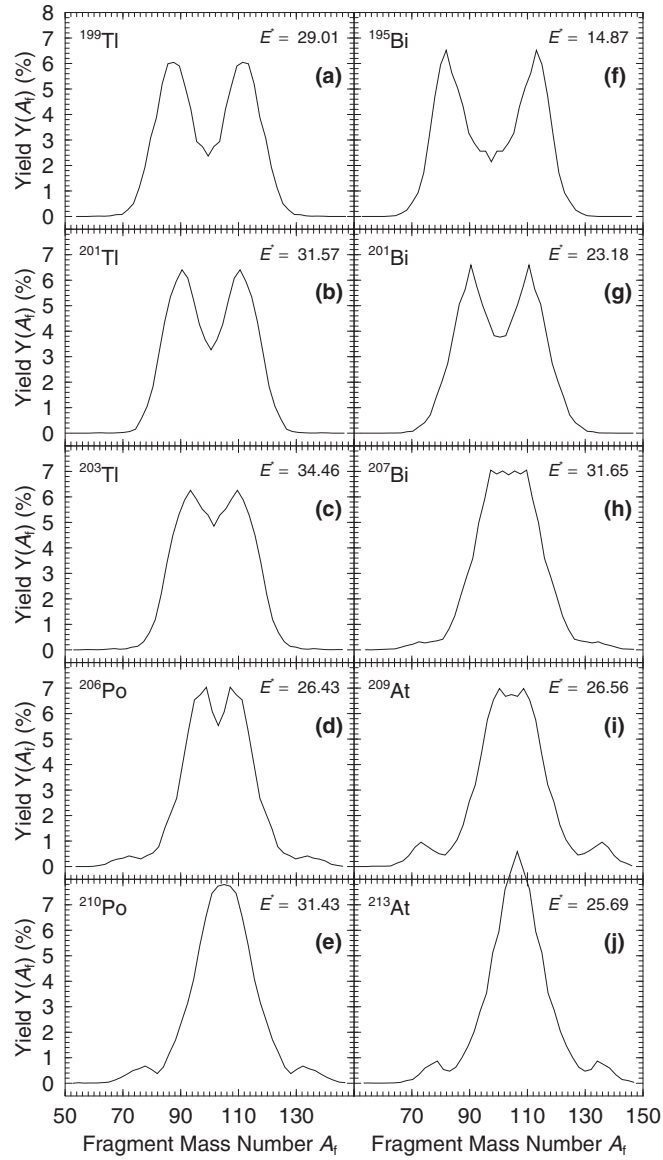

FIG. 2. Calculated fission-fragment mass yields for 10 isotopes of Tl, Bi, Po, and At. The compound-nucleus excitation energies E^* are in units of MeV. Details of these distributions are discussed in the text.

a split with a heavy fragment nucleon number $A = 132$. The lighter fragment would then be much smaller than the smaller fragment in actinide fission. We found a suitable candidate would be ^{196}W. In Figs. 1(a), 1(b), and 1(c) we show the calculated yields for ^{186}W, ^{190}W, and ^{196}W, respectively. There is indeed a small peak near $A = 132$ for ^{196}W, but it is not very prominent at 0.91%. In ^{190}W it is slightly more developed at 1.78% but fairly minimal in the β-stable isotope ^{186}W. One may wonder why the magicity of ^{132}Sn is much less expressed here than in the actinides. One reason is that the macroscopic energy is much more dominant here. Also with the energy chosen, some of the shell effect is damped out. We have made a calculation at 33 MeV for ^{190}W, which is more easily reachable experimentally than ^{196}W. At this lower excitation energy the influence of the shell effects are more significant with the $A = 132$ peak much higher at 3.86%. The yield for fission at this energy is shown as a dashed line in Fig. 1(b). Figure 2 shows yields for selected other isotopes.

We will return to discuss the results in Figs. 1 and 2 further, but first we introduce a summary of our results in "nuclear-chart" format. In Fig. 3 we show the ratio between the calculated yield at symmetry and the maximum on the yield curve. Often it is the inverse, "peak-to-valley" ratio that is used [40], but since the valley yield occasionally can be zero in our calculations we use the inverse measure. In Fig. 3 well-developed asymmetric yields therefore correspond to low values of this ratio. It is quite obvious from the figure that our results show a contiguous region of asymmetric fission in the neutron-deficient Pb region, the "southwest" quadrant with respect to

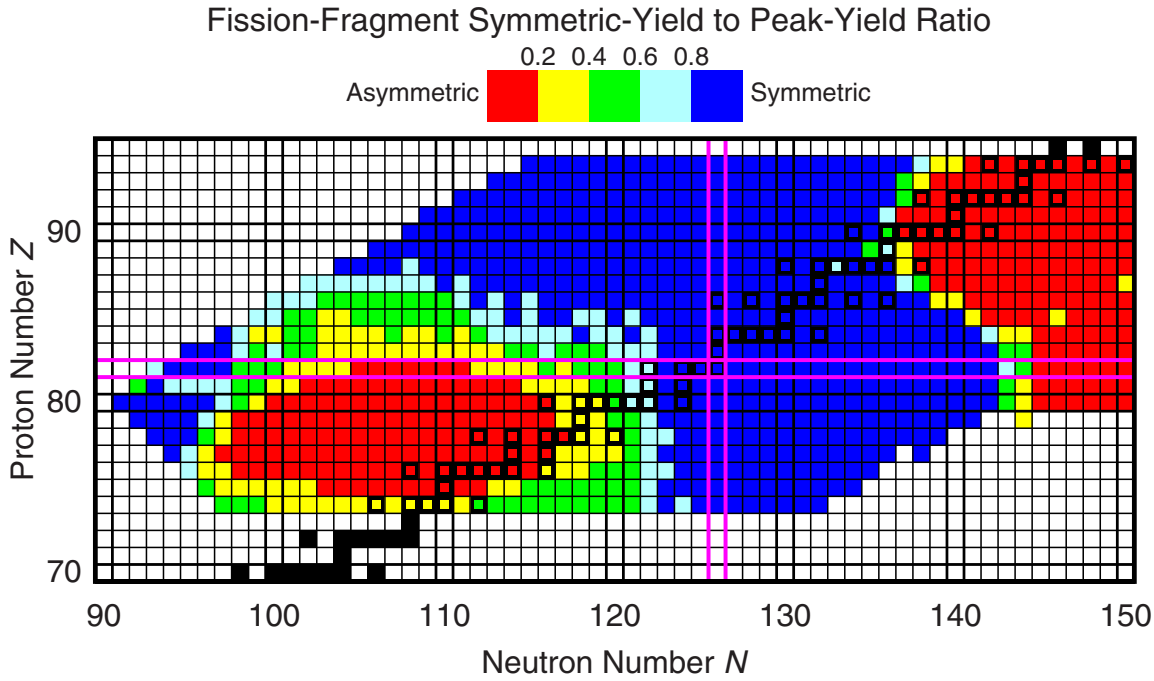

FIG. 3. (Color online) Calculated symmetric-yield to peak-yield ratios for 987 fissioning systems. Black squares (open in colored regions, filled outside) indicate β-stable nuclei. We find a new, contiguous region of asymmetric fission separated from the classical location of asymmetric fission in the actinides by an extended area of symmetric fission.

^{208}Pb. Currently there are only limited data in this region. It has been firmly established that following electron capture on ^{180}Tl the daughter ^{180}Hg fissions into fragments with mass distributions centered at $A = 80$ and $A = 100$ [1,5]. Figures 3 and 4 show that ^{178}Hg is also predicted to fission asymmetrically. This is consistent with what was observed in β-delayed fission of ^{178}Hg following electron capture on ^{178}Tl [4], although the number of data points is very small. The calculated yields on which Figs. 3 and 4 are based are in Ref. [41].

Itkis and collaborators have studied fission-fragment mass distributions of a number of nuclides near $Z = 80$ and $A = 200$ at about 10 MeV above the saddle energy [36,37]. They are $^{187}_{77}$Ir, $^{189}_{77}$Ir, $^{195}_{79}$Au, $^{198}_{80}$Hg, $^{201}_{81}$Tl, $^{207}_{83}$Bi, $^{210}_{84}$Po, and $^{213}_{85}$At. For the first four cases, $^{187}_{77}$Ir, $^{189}_{77}$Ir, $^{195}_{79}$Au, and $^{198}_{80}$Hg, the experimental yields are symmetric but the yield curves become increasingly flat in the symmetric region as the nucleon number increases. We obtain asymmetric yields for these four cases. We do not show in any figure the calculated yields for the Ir isotopes (but they can be found in the supplemental information in Ref. [41]) but we show in Figs. 1(d) and 1(i) the calculated yields for ^{195}Au and ^{198}Hg. It is interesting to establish whether the differences between the predicted and measured character of the yields are merely isolated failures of the model or reflect a more general shortcoming in this region of the nuclear chart. One possibility is that the global theoretical picture is realistic, but that it fails to describe the exact location of the transition between symmetric and asymmetric fission. This is analogous to the difficulties all global nuclear-structure models have, to some degree, in describing the exact location of the transition between spherical nuclei near magic numbers and deformed nuclei [42]. We note that we find the transition point to symmetry at quite nearby nuclei that differ from these two isotopes by only a few neutron orbitals; the calculated yields for ^{201}Au in Fig. 1(e) and ^{202}Hg in Fig. 1(j) are symmetric.

Another possible reason for the differences between calculated and measured yields is that the potential-energy surface is inaccurate in this region of nuclei. It is known that the masses, calculated in the identical model, show large discrepancies with respect to experimental masses near $^{96}_{40}$Zr$_{56}$ with calculated masses almost 2 MeV too high [43]. These are some of the largest deviations occurring in the calculated mass table. The reason is that in experimental results the spherical neutron $N = 56$ subshell gap widens near proton number $Z = 40$ [44]. No current global model obtains such an effect leading to a changing magnitude of a spherical neutron level gap for minor changes of the proton number, when the shape remains spherical. For $N = 56$ this is an experimentally observed effect. Since the calculated $N = 56$ subshell gap is too small, the end result is that the calculated masses for some nuclei are too high by up to 2 MeV. For the fission potential-energy surface, for regions corresponding to symmetric division leading to two fragments in this region, this means that the calculated potential energy could be too high by 4 MeV. This might be sufficient to result in a low calculated symmetric yield in this region, and the differences with respect to experiment might be confined to this localized region just as it the case for the nuclear mass model near $^{96}_{40}$Zr$_{56}$ [43].

The calculated yields for $^{201}_{81}$Tl, $^{207}_{83}$Bi, $^{210}_{84}$Po, and $^{213}_{85}$At, shown in Figs. 2(b), 2(h), 2(e), and 2(j), agree well with observations, which find symmetric fragment distributions for these nuclides. Figures 1 and 2 display yields for additional isotopes for each of these elements to illustrate how quickly the structure of the yield curves can change with neutron number. For example, in Fig. 1(g) fission of ^{176}Hg is symmetric,

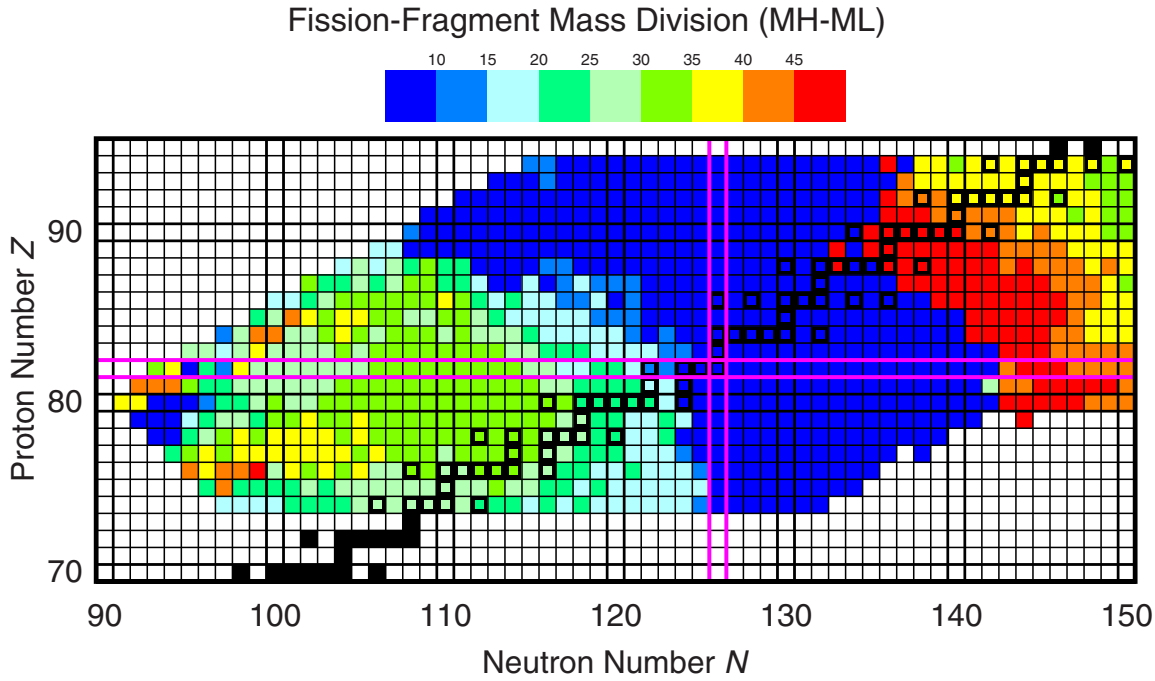

FIG. 4. (Color online) Calculated mass difference between location of the heavy mass-yield peak and the light mass-yield peak.

whereas in ^{180}Hg, which is just four neutrons heavier, a strong asymmetry has developed.

Figures 3 and 4 also tell us about the location of the transition between symmetric fission and asymmetric fission in the heaviest region in the "northeast" quadrant, with respect to ^{208}Pb. Since we (and others) only roughly define what is meant by "transition point," the discussion is somewhat approximate. The exact details are in the figures and in the 987 calculated yield curves [41]. In Ref. [12] it is stated that the mass number has a "decisive influence" on the mass asymmetry of fission and that for all nuclei with $A < 226$ symmetric fission has been found to prevail. However, in the paper there is only data on both sides of the transition between symmetry and asymmetry for two isotope chains, namely for the $Z = 91$ and $Z = 90$ isotope chains. In our opinion this is a too firm conclusion about the location of the transition, since data is available on both sides of the transition line for only these two chains out of the 10 different elements ($84 < Z < 95$). In Fig. 3 the calculated transition agrees well for these two elements. In the experimental data the heaviest isotope available in the $Z = 89$ chain is ^{226}Ac for which symmetric fission is clearly dominant in the yield curve, so here the statement should be that all isotopes with $A < 227$ fission symmetrically. But the statement, although correct, is somewhat misleading because if data for additional, heavier, isotopes became available it might show that some of them fission symmetrically. In our calculations the transition between symmetric and asymmetric fission occurs to good accuracy at $A = 226$ in the range $84 < Z < 92$ but experimental data showing the transition point is lacking for all elements except Th and Pa. But based on our calculated results we can make the interesting observation that above $Z = 90$ the calculated transition between symmetry and asymmetry now takes place along constant $N - Z \approx 47$ rather than constant A. There are no experiments available for U, Np, and Pu in this transition region. Experiments at low energy would be difficult but we propose attempts be made to locate the transition point along these isotope sequences.

Also interesting is the difference between the locations of the heavy-mass and light-mass peaks shown in Fig. 4. In the actinide region there is a systematic decrease in this calculated mass difference with increasing mass of the fissioning nuclei. This is very consistent with experimental data. It is well known that in actinide fission the mass of the heavy-yield peak is relatively constant at $A \approx 140$, independently of compound-system mass number. The light-mass peak then by necessity moves from lighter towards heavier-mass numbers and the mass difference between the peaks decreases with increasing fissioning compound-nucleus mass number.

IV. SUMMARY

We have calculated and characterized the fission-fragment mass yield for 987 nuclides in the region $74 \leqslant Z \leqslant 94$ and $91 \leqslant N \leqslant 150$. We have determined the extension of the new region of asymmetry whose first member, ^{180}Hg, was discovered only a few years ago [1]. We found a contiguous region of asymmetry comprising roughly 200 nuclides. We find agreement between our results and some of the experimental data in this region and differences for some other experimental data. But at this point the experimental data are too scarce with only ten or so data sets available, sometimes with very limited statistics, to permit major conclusions to be drawn with confidence. Now that we have predicted an extended region of asymmetric fission it is possible to test this prediction by studying fission yields for a sufficiently large number of nuclides located across the region, so that reliable conclusions can be drawn. Also of high interest is to study the yields as functions of compound-nucleus excitation energy.

In the actinide region we calculate that $A \approx 226$ is the transition line between symmetric and asymmetric fission between $84 \leqslant Z \leqslant 90$. For higher Z we find that the transition between symmetric and asymmetric fission occurs along $N - Z \approx 47$, a prediction that still has to be tested experimentally.

ACKNOWLEDGMENTS

We acknowledge generous comments on the manuscript and results by A. N. Andreyev, T. Ichikawa, A. Iwamoto, K. Nishio, and A. J. Sierk. This work was supported by travel grants to JAEA from the Reimei Research Program of Advanced Science Research Center, Japan Atomic Energy Agency. This work was carried out under the auspices of the National Nuclear Security Administration of the U.S. Department of Energy at Los Alamos National Laboratory under Contract No. DE-AC52-06NA25396 (P.M.). J.R. was supported by the Office of Nuclear Physics in the U.S. Department of Energy's Office of Science under Contract No. DE-AC02-05CH11231.

[1] A. N. Andreyev, J. Elseviers, M. Huyse, P. Van Duppen, S. Antalic, A. Barzakh, N. Bree, T. E. Cocolios, V. F. Comas, J. Diriken, D. Fedorov, V. Fedosseev, S. Franchoo, J. A. Heredia, O. Ivanov, U. Köster, B. A. Marsh, K. Nishio, R. D. Page, N. Patronis, M. Seliverstov, I. Tsekhanovich, P. Van den Bergh, J. Van De Walle, M. Venhart, S. Vermote, M. Veselsky, C. Wagemans, T. Ichikawa, A. Iwamoto, P. Möller, and A. J. Sierk, Phys. Rev. Lett. **105**, 252502 (2010).

[2] A. N. Andreyev, S. Antalic, D. Ackermann, L. Bianco, S. Franchoo, S. Heinz, F. P. Heßberger, S. Hofmann, M. Huyse, Z. Kalaninová, I. Kojouharov, B. Kindler, B. Lommel, R. Mann, K. Nishio, R. D. Page, J. J. Ressler, B. Streicher, S. Saro, B. Sulignano, and P. Van Duppen, Phys. Rev. C **87**, 014317 (2013).

[3] J. F. W. Lane, A. N. Andreyev, S. Antalic, D. Ackermann, J. Gerl, F. P. Heßberger, S. Hofmann, M. Huyse, H. Kettunen, A. Kleinböhl, B. Kindler, I. Kojouharov, M. Leino, B. Lommel, G. Münzenberg, K. Nishio, R. D. Page, Š. Šáro, H. Schaffner, M. J. Taylor, and P. Van Duppen, Phys. Rev. C **87**, 014318 (2013).

[4] V. Liberati, A. N. Andreyev, S. Antalic, A. Barzakh, T. E. Cocolios, J. Elseviers, D. Fedorov, V. N. Fedoseeev, M. Huyse, D. T. Joss, Z. Kalaninová, U. Köster, J. F. W. Lane, B. Marsh, D. Mengoni, P. Molkanov, K. Nishio, R. D. Page, N. Patronis, D. Pauwels, D. Radulov, M. Seliverstov, M. Sjödin, I. Tsekhanovich, P. Van den Bergh, P. Van Duppen, M. Venhart, and M. Veselský, Phys. Rev. C **88**, 044322 (2013).

[5] J. Elseviers, A. N. Andreyev, M. Huyse, P. Van Duppen, S. Antalic, A. Barzakh, N. Bree, T. E. Cocolios, V. F. Comas, J. Diriken, D. Fedorov, V. N. Fedosseev, S. Franchoo, L. Ghys, J. A. Heredia, O. Ivanov, U. Köster, B. A. Marsh, K. Nishio, R. D. Page, N. Patronis, M. D. Seliverstov, I. Tsekhanovich, P. Van den Bergh, J. Van De Walle, M. Venhart, S. Vermote, M. Veselský, and C. Wagemans, Phys. Rev. C **88**, 044321 (2013).

[6] K.-H. Schmidt and B. Jurado, JEF/DOC 1423, NEA of OECD, Paris, 2011 (unpublished).

[7] http://www.cenbg.in2p3.fr/GEF, http://www.khs-erzhausen.de.

[8] J. Randrup and P. Möller, Phys. Rev. Lett. **106**, 132503 (2011).

[9] J. Randrup, P. Möller, and A. J. Sierk, Phys. Rev. C **84**, 034613 (2011).

[10] J. Randrup and P. Möller, Phys. Rev. C **88**, 064606 (2013).

[11] P. Möller, J. Randrup, and A. J. Sierk, Phys. Rev. C **85**, 024306 (2012).

[12] K.-H. Schmidt, S. Steinhäuser, C. Böckstiegel, A. Grewe, A. Heinz, A. R. Junghans, J. Benlliure, H.-G. Clerc, M. de Jong, J. Müller, M. Pfützner, and B. Voss, Nucl. Phys. A **665**, 221 (2000).

[13] L. Ghys, A. N. Andreyev, M. Huyse, P. Van Duppen, S. Sels, B. Andel, S. Antalic, A. Barzakh, L. Capponi, T. E. Cocolios, X. Derkx, H. De Witte, J. Elseviers, D. V. Fedorov, V. N. Fedosseev, F. P. Hessberger, Z. Kalaninová, U. Köster, 14 J. F. W. Lane, V. Liberati, K. M. Lynch, B. A. Marsh, S. Mitsuoka, P. Möller, Y. Nagame, K. Nishio, S. Ota, D. Pauwels, R. D. Page, L. Popescu, D. Radulov, M. M. Rajabali, J. Randrup, E. Rapisarda, S. Rothe, K. Sandhu, M. D. Seliverstov, A. M. Sjödin, V. L. Truesdale, C. Van Beveren, P. Van den Bergh, Y. Wakabayashi, and M. Warda, Phys. Rev. C **90**, 041301 (2014).

[14] K. T. R. Davies, A. J. Sierk, and J. R. Nix, Phys. Rev. C **13**, 2385 (1976).

[15] A. J. Sierk, S. E. Koonin, and J. R. Nix, Phys. Rev. C **17**, 646 (1978).

[16] J. Błocki, Y. Boneh, J. R. Nix, J. Randrup, M. Robel, A. J. Sierk, and W. J. Swiatecki, Ann. Phys. (N.Y.) **113**, 330 (1978).

[17] A. J. Sierk and J. R. Nix, Phys. Rev. C **21**, 982 (1980).

[18] H. A. Kramers, Physica (Amsterdam) **7**, 284 (1940).

[19] P. Grangé, H. C. Pauli, and H. A. Weidenmüller, Phys. Lett. B **88**, 9 (1979).

[20] H. Hofmann and J. R. Nix, Phys. Lett. B **122**, 117 (1983).

[21] P. Grangé, L. Jun-Qing, and H. A. Weidenmüller, Phys. Rev. C **27**, 2063 (1983).

[22] J. R. Nix, A. J. Sierk, H. Hofmann, F. Scheuter, and D. Vautherin, Nucl. Phys. A **424**, 239 (1984).

[23] F. Scheuter, C. Grégroire, H. Hofmann, and J. R. Nix, Phys. Lett. B **149**, 303 (1984).

[24] Y. Abe, S. Ayik, P.-G. Reinhard, and E. Suraud, Phys. Rep. **275**, 49 (1996).

[25] P. Fröbrich and I. I. Gontchar, Phys. Rep. **292**, 131 (1998).

[26] D. V. Vanin, G. I. Kosenko, and G. D. Adeev, Phys. Rev. C **59**, 2114 (1999).

[27] A. V. Karpov, P. N. Nadtochy, D. V. Vanin, and G. D. Adeev, Phys. Rev. C **63**, 054610 (2001).

[28] G. Chaudhuri and S. Pal, Phys. Rev. C **63**, 064603 (2001).

[29] P. N. Nadtochy, G. D. Adeev, and A. V. Karpov, Phys. Rev. C **65**, 064615 (2002).

[30] P. N. Nadtochy, A. Kelić, and K.-H. Schmidt, Phys. Rev. C **75**, 064614 (2007).

[31] Y. Aritomo, K. Hagino, K. Nishio, and S. Chiba, Phys. Rev. C **85**, 044614 (2012).

[32] Y. Aritomo and S. Chiba, Phys. Rev. C **88**, 044614 (2013).

[33] Y. Aritomo, S. Chiba, and F. Ivanyuk, Phys. Rev. C **90**, 054609 (2014).

[34] T. Ichikawa, A. Iwamoto, P. Möller, and A. J. Sierk, Phys. Rev. C **86**, 024610 (2012).

[35] A. N. Andreyev M. Huyse, and P. Van Duppen, Rev. Mod. Phys. **85**, 1541 (2013).
[36] M. G. Itkis, N. A. Kondrat'ev, S. I. Mul'gin, V. N. Okolovich, A. Ya. Rusanov, and G. N. Smirenkin, Yad. Fiz. **52**, 944 (1990).
[37] M. G. Itkis, N. A. Kondrat'ev, S. I. Mul'gin, V. N. Okolovich, A. Ya. Rusanov, and G. N. Smirenkin, Yad. Fiz. **53**, 1225 (1991).
[38] P. Möller, A. J. Sierk, T. Ichikawa, A. Iwamoto, R. Bengtsson, H. Uhrenholt, and S. Åberg, Phys. Rev. C **79**, 064304 (2009).
[39] P. Möller, A. J. Sierk, T. Ichikawa, A. Iwamoto, and M. Mumpower, Phys. Rev. C **91**, 024310 (2015).
[40] R. Vandenbosch and J. R. Huizenga, *Nuclear Fission* (Academic Press, New York, 1973).
[41] See Supplemental Material at http://link.aps.org/supplemental/10.1103/PhysRevC.91.044316 for calculated yields on which Figs. 3 and 4 are based.
[42] S. Raman, C. W. Nestor, Jr., and P. Tikkanen, Atomic Data Nucl. Data Tables **78**, 1 (2001).
[43] P. Möller, J. R. Nix, W. D. Myers, and W. J. Swiatecki, Atomic Data Nucl. Data Tables **59**, 185 (1995).
[44] R. Bengtsson, P. Möller, J. R. Nix, and J.-Y. Zhang, Phys. Scr. **29**, 402 (1984).